catalysts

MDPI

Article

Transfer Hydrogenation of Biomass-Like Phenolic Compounds and 2-PrOH over Ni-Based Catalysts Prepared Using Supercritical Antisolvent Coprecipitation

Alexey Philippov *, Nikolay Nesterov and Oleg Martyanov

Boreskov Institute of Catalysis, Siberian Branch of the Russian Academy of Sciences, Academician Lavrentiev Avenue 5, 630090 Novosibirsk, Russia

* Correspondence: philippov@catalysis.ru; Tel.: +7-38-3326-9313

Abstract: Transfer hydrogenation (TH) is considered as one of the most promising ways to convert biomass into valuable products. This study aims to demonstrate the performance of high-loaded Ni-based catalysts in the TH of phenolic compounds such as guaiacol and dimethoxybenzenes. The experiments were carried out under supercritical conditions at 250 °C using 2-PrOH as the only hydrogen donor. Ni-SiO_2 and NiCu-SiO_2 were synthesized using the eco-friendly original method based on supercritical antisolvent coprecipitation. It has been found that guaiacol is rapidly converted into 2-methoxycyclohexanol and cyclohexanol, while the presence of Cu impedes the formation of the latter product. Transformations of dimethoxybenzene position isomers are slower and result in different products. Thus, 1,3-dimethoxybenzene loses oxygen atoms transform into methoxycyclohexane and cyclohexanol, whereas the saturation of the aromatic ring is more typical for other isomers. The Cu addition increases specific catalytic activity in the TH of 1,2-and 1,3-dimethoxybenzene compared to the Cu-free catalyst.

Keywords: transfer hydrogenation; antisolvent supercritical coprecipitation; phenolic compounds; 2-propanol; hydrodeoxygeantion; hydrodearomatization

Citation: Philippov, A.; Nesterov, N.; Martyanov, O. Transfer Hydrogenation of Biomass-Like Phenolic Compounds and 2-PrOH over Ni-Based Catalysts Prepared Using Supercritical Antisolvent Coprecipitation. *Catalysts* **2022**, *12*, 1655. https://doi.org/10.3390/catal12121655

Academic Editors: Linda Zh Nikoshvili, Lioubov Kiwi-Minsker and Valentin Yu Doluda

Received: 23 November 2022
Accepted: 14 December 2022
Published: 15 December 2022

1. Introduction

The global energy crisis, accompanied by environmental issues, is driving society to the need for a green transition. In this concept, lignocellulosic biomass should play the role of the renewable and non-edible source of carbon atoms [1,2]; therefore, its conversion into chemicals, materials, and fuels is widely studied [3,4]. Unlike cellulose, lignin has an irregular structure represented by phenolic fragments that makes lignin upgrading into valuable products difficult. Due to the high oxygen content reaching up to 40 wt.% [5], hydrodeoxygenation (HDO) via H_2 hydrogenation is considered as one of the most promising and effective methods of lignin transformations [6,7]. However, this method has important disadvantages from practical and environmental points of view. First, H_2 is known for its corrosive activity and explosiveness, and it requires high-pressure equipment presenting a significant safety hazard. Second, the low solubility of molecular hydrogen in almost all organic compounds results in low rates of hydrogenation in the liquid phase. At the same time, the use of organic solvents prevents biomass thermal decomposition and increases the effectiveness of the whole process [8].

Alcohols can be easily produced from renewable sources; moreover, they demonstrate the excellent H-donor activity in transfer hydrogenation (TH). For example, alcohols were used as H-donors in the TH of phenol-like compounds [9–11] and other bio-based molecules [12,13]. Sometimes alcohols demonstrate superior H-donor activity compared to H_2 [1,14]; however, as a rule, the use of organic H-donors requires harder conditions, including supercritical fluids [15,16]. In addition to donor activity, the supercritical state of alcohols also promotes the destruction of complex compounds such as lignin, polymers,

or inorganic oxides [17–19]. Thus, supercritical alcohols are considered as a promising reducing agents for H_2-free hydrogenation.

Biomass catalytic conversion is aimed at obtaining a huge number of products, and heterogeneous catalysts are considered as an essential part of the process. One of the promising methods of the catalyst preparation is supercritical antisolvent (SAS) coprecipitation, which demonstrated promising results in the preparation of metal nanoparticles [10,20,21]. This method is based on high supersaturation of a precursor solution with supercritical fluid, in the role of which CO_2 is often used. The formation of a CO_2-solvent binary system results in a sharp decrease in dissolving power and the fast precipitation of catalyst precursors [22], which can be coprecipitated simultaneously with oxide sols, forming a catalyst support [21]. One of the key advantages of the SAS coprecipitation method is that it allows metal in a catalyst to reach up to 90% while maintaining the high dispersion of the metal particles [23,24]. Moreover, CO_2 and a solvent of the precursors can be easily separated and used repeatedly in a way that complies with the principals of green chemistry. In our earlier studies, the high-loaded nickel-based catalysts prepared according SAS coprecipitation demonstrated excellent results in the TH of anisole [10,25].

Considering the potential of supercritical fluids in catalyst preparation and H_2-free hydrogenation, this study aims to demonstrate the performance of the high-loaded Ni-based catalysts in the transfer hydrogenation of phenolic compounds, such as guaiacol and dimethoxybenzenes, for the first time. For this, the catalysts were synthesized accordingly the supercritical antisolvent coprecipitation method using sc-CO_2 as an antisolvent. The obtained catalysts containing 36–40 wt.% of nickel were used in the TH of guaiacol and dimethoxybenzenes modeling the products of lignin degradation. The transformations were carried out in sc-2-PrOH, which played the role of a solvent and an H-donor. Special attention was paid to the effect of copper addition to nickel and the comparison of guaiacol and dimethoxybenezene positional isomers in terms of their reactivity and the selectivity of their transformations.

2. Results

2.1. Catalyst Properties

The properties of the synthesized catalysts are described in detail in our previous study [25] and in the Supplementary Materials. Briefly, the results of XRF demonstrate that the Ni-SiO_2 catalyst contains 36.4 wt.% of Ni, while NiCu-SiO_2 contains 40.7 wt.% and 4.0 wt.% of nickel and copper, respectively (Table S1). XRD shows that Ni^0 and Cu^0 form the monophasic particles, which means the crystallite size does not exceed 5.5 nm, while the mean size of Ni^0 crystallites in Ni-SiO_2 is 6.0 nm (Figure S1). The samples have similar areas of Ni atoms measured by CO adsorption–35 m^2/g and 32 m^2/g for Ni-SiO_2 and NCu-SiO_2, respectively. TEM microphotographs shows that the nanosized particles are agglomerated in larger structures up to several micrometers in size (Figure S2). EDX data show that Ni and Cu are evenly distributed.

2.2. Transfer Hydrogenation of Guaiacol

Both catalysts provide higher conversion in TH of guaiacol than the other phenolic compounds used in this study. Guaiacol has a free OH group, which facilitates the interaction between this substrate and the catalyst surface according to the literature data [9,26]. The conversion of guaiacol reaches 100% after 2 h, and Ni-SiO_2, 2-methoxycyclohexanol, and cyclohexanol are found to be the main products (Figure 1). The kinetic data show that 2-methylcyclohexanol formed in the reaction mixture transforms into cyclohexanol and cyclohexane. In our recent study [25], methoxycyclohexane formed after the aromatic ring saturation of anisole demonstrated stability under very similar conditions. Thus, we suggest that the presence of two oxygen atoms in the substrate as well as the free OH group can facilitate hydrodeoxygenation.

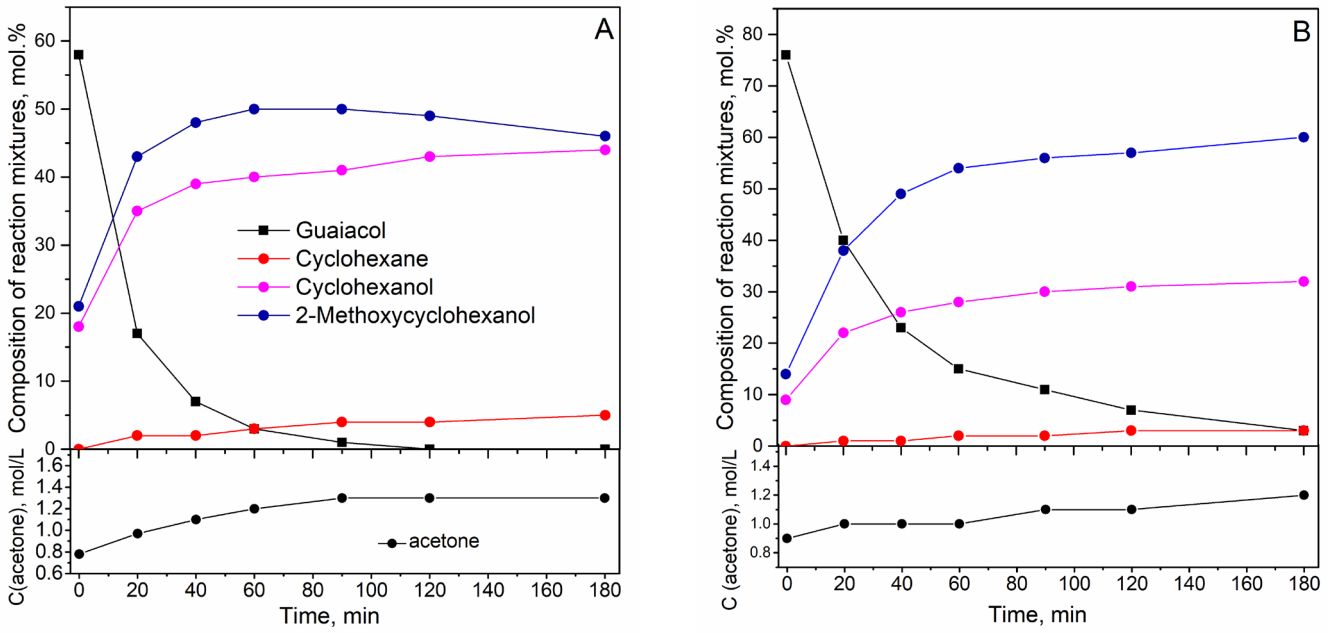

Figure 1. The composition of the reaction mixture in the course of guaiacol transformation over catalysts: (**A**)–Ni-SiO_2 and (**B**)–NiCu-SiO_2. 250 °C, 7.0–7.7 MPa, and m(catalyst) = 0.10–0.11 g.

The literature data show that the addition of Cu to Ni nanoparticles can improve the catalytic performance of the Ni-based catalysts. It has been demonstrated that Cu lowers the catalyst activation temperature [23,27] and contributes to the resistance of the Ni-Cu phase against oxidation [28,29]. Moreover, the presence of Cu can promote anisole HDO when H_2 is used [24,30]. However, in case of transfer hydrogenation, the Cu additives decrease the conversion of anisole as well as the rate of C-O bond cleavage [25]. These observations were confirmed in the present study because the use of NiCu-SiO_2 results in the lower guaiacol conversion compared to Ni-SiO_2 catalyst (Figure 1). At the same time, the cyclohexanol yield reaches only 32% vs. 44% after 3 h over NiCu-SiO_2 and Ni-SiO_2, respectively. Our previous studies demonstrated that this effect is based on acetone formation, which is suggested to adsorb on the catalyst surface, blocking active sites [25]. It is clearly seen in Figure S3 (see the Supplementary Materials) that the logarithmic dependence of guaiacol conversion on time is not linear.

2.3. Transfer Hydrogenation of Dimethoxybenzenes

The conversion of 1,2-dimethoxybenzene (1,2-DMB) achieves 83% and 88% for 3 h over Ni-SiO_2 and NiCu-SiO_2, respectively (Figure 2). In both cases, 1,2-dimethoxycyclohexane was found to be the main product, whereas the concentrations of other compounds did not exceed 10%. Thus, the oxygen-containing groups are almost uninvolved in the TH, in contrast to the results obtained for guaiacol. The difference can be related to the influence of OH group of guaiacol, which interacts with the catalyst facilitating the adsorption of the organic molecule. This promotes the transformations of the oxygen-containing groups on the catalyst surface. It is important to notice that the Cu addition results in the higher rate constant (Table 1) as well as the specific catalytic activity (Table 2), compared to the Cu-free catalyst. This fact is in good accordance with the known literature data [14,26,31] demonstrating the positive Cu influence on HDO under TH conditions.

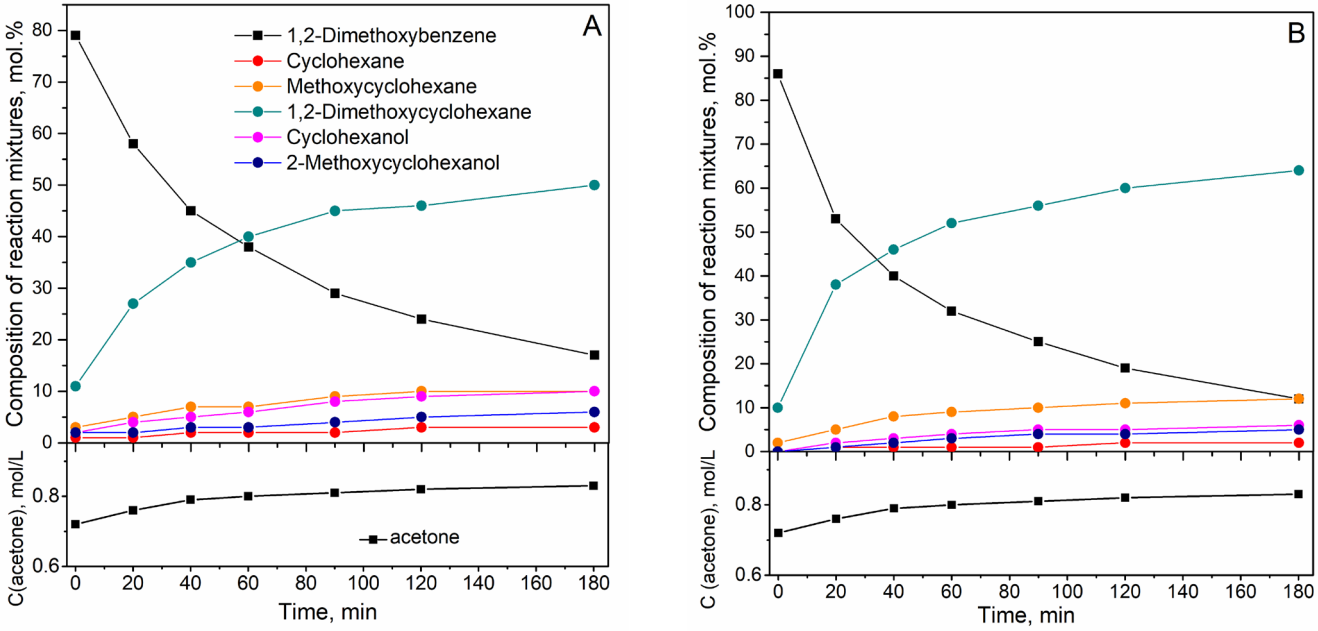

Figure 2. The composition of the reaction mixture in the course of 1,2-dimethoxybenzene (1,2-DMB) transformation over (**A**)–Ni-SiO_2 and (**B**)–NiCu-SiO_2. 250 °C, 7.0–7.7 MPa, and m(catalyst) = 0.10–0.11 g.

Table 1. Rate constants of phenolic compound transformations in TH with 2-PrOH, 250 °C, and 7.0–7.7 MPa. All constants were calculated taking into account the negative influence of acetone.

Catalyst	$k \times 10^{-2}$, min^{-1}			
	Guaiacol	1,2-DMB	1,3-DMB	1,4-DMB
Ni-SiO_2	5.9	1.3	0.65	1.3
NiCu-SiO_2	2.6	1.6	0.67	0.71

Table 2. Specific activity of the catalysts in TH of phenolic compounds at 250 °C.

Catalyst	$k/S_{CO} \times 10^{-3}$, $min^{-1} \times m^{-2}$				
	S_{CO}, m^2/g	Guaiacol	1,2-DMB	1,3-DMB	1,4-DMB
Ni-SiO_2	35	15	3.4	1.7	3.4
NiCu-SiO_2	32	7.4	4.5	1.9	2.0

Figure 3 shows the data obtained in the experiments with 1,3-dimethoxybenzene (1,3-DMB). After 3 h at 250 °C, the conversion of the initial substrate is relatively low and reaches 44% and 52% over the Ni-SiO_2 and NiCu-SiO_2 catalyst, respectively. In terms of the rate constants and the specific catalytic activity, the Cu addition has a limited positive effect (Tables 1 and 2). The qualitative content of the products has the significant differences compared to 1,2-DMB. Methoxycyclohexane and cyclohexanol were found to be the main products; at the same time, oxygen-free cyclohexane is presented in small amounts. Thus, the saturation of the 1,3-DMB benzene ring under TH conditions is always accompanied by C-O cleavage that is not typical for other phenolic compounds used in this study. Unfortunately, reductive transformations of 1,3-DMB are not widely studied in the literature; however, the results of the conventional hydrogenation of 1,3-DMB over silica-supported Pt and Pd [32] catalysts are quite similar to the data presented here.

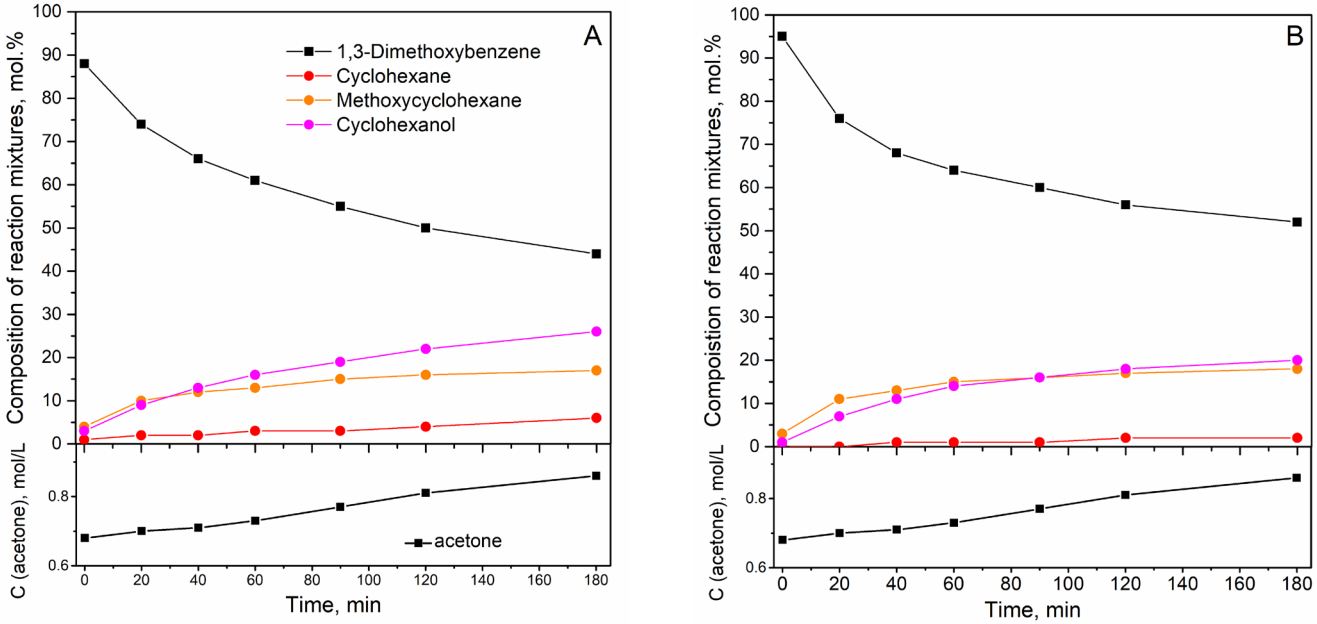

Figure 3. The composition of the reaction mixture in the course of 1,3-dimethoxybenzene (1,3-DMB) transformation over catalysts: (**A**)–Ni-SiO_2 and (**B**)–NiCu-SiO_2. 250 °C, 7.0–7.7 MPa, and m(catalyst) = 0.10–0.11 g.

In contrast to other position isomers, Cu negatively affects both the rate constant of 1,4-DMB consumption and the specific catalytic activity (Tables 1 and 2). This fact is mirrored in the conversion of 1,4-DMB, which reaches 84% and 49% over the Ni-SiO_2 and NiCu-SiO_2 catalysts, respectively (Figure 4). Thus, it is clearly seen that the influence of Cu on rate constants changes from positive for 1,2-DMB to almost neutral and negative for 1,3-DMB and 1,4-DMB, respectively. We assume that this effect can be related to the more effective adsorption of 1,2-DMB promoted by Cu. For example, De Castro et al. [26] explain the low reactivity of 3-methoxyphenol and 4-methoxyphenol in TH in terms of the adsorption on the catalyst surface. The results of the FTIR study provided by the authors demonstrated that after dissociation of the OH group, tilted structures are formed. The oxygen-containing groups of 2-methoxycyclohexanol are closer to the Ni surface compared to other derivatives, which causes the faster transformation of 2-methoxycyclohexanol. This fact, along with the known promoting effect of Cu on the adsorption of oxygen-containing compounds [31,33], proves our observations.

The transfer hydrogenation of 1,4-DMB results in the formation 1,4-dimethoxycyclohexane and 4-methoxycyclohexanol (Figure 4). Small amounts of methoxycyclohexane, cyclohexanol, and cyclohexane have been also found in the reaction mixtures. Figure 4 shows that the Cu addition affects the yields of the products negatively; however, the selectivity remains almost unchanged. As seen, the C_{arom}-O bonds are not significantly involved in the reductive transformations in contrast to the aromatic rings. At the same time, the formation of 4-methoxycyclohexanol indicates the noticeable activity of both catalysts in the CH_3-O bond cleavage.

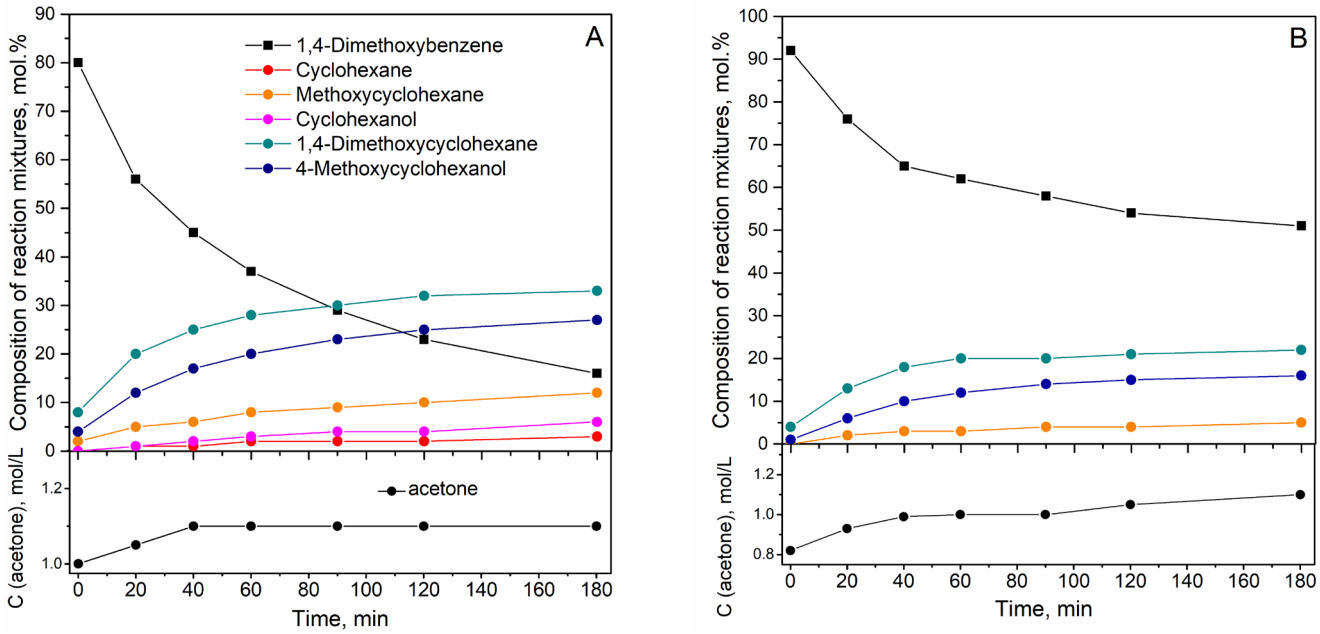

Figure 4. The composition of the reaction mixture in the course of 1,4-dimethoxybenzene (1,4-DMB) transformation over catalysts: (**A**)–Ni-SiO_2 and (**B**)–NiCu-SiO_2. 250 °C, 7.0–7.7 MPa, and m(catalyst) = 0.10–0.11 g.

2.4. Kinetic Studies

As it was mentioned above, the first-order kinetic model as well as any other models based on the higher-order kinetic equations of the elementary reaction do not fit the experimental data (see Supplementary Materials). In our recent study devoted to anisole transformations in the TH [25], the negative influence of acetone was demonstrated. In the kinetic calculations, it was mirrored as a negative term $k_{ac} \times C_{ac}$ (Equation (3)), decreasing the rate constant. This term includes $k_{ac,}$ which is technically the quasi-equilibrium constant showing the ratio between acetone adsorbed on the catalysts surface and in the solution. The same kinetic model applied to guaiacol and dimethoxybenzenes describes the dependence of conversion on time quite well (see the Supplementary Materials).

The calculated rate constants (Table 1) show that the transformation of guaiacol over Ni-SiO_2 occurs at least 4.5 times faster than for dimethoxybenzenes. The Cu addition has a negative effect on the guaiacol conversion; therefore, the difference in the kinetic constants over NiCu-SiO_2 is not so high. However, in the case of 1,2-DMB copper increases the rate constant from 3.4×10^{-3} min^{-1} m^{-2} to 4.5×10^{-3} min^{-1} m^{-2}. Additionally, the limited positive effect of the copper addition on the rate constant was found for 1,3-DMB. To calculate the specific catalytic activity, the rate constants were normalized to the Ni^0 surface area (Table 2). Due to the close values of the Ni^0 area, the dependences observed for the rate constants are also valid for the specific catalytic activity.

The comparison of the data obtained in this study [25] shows that the specific catalytic activity in anisole transformation reaches 9.0×10^{-3} min^{-1} m^{-2} and 3.8×10^{-3} min^{-1} m^{-2} for the Ni-SiO_2 and NiCu-SiO_2 catalysts, respectively. Thus, the influence of copper on anisole TH is close to those observed for guaiacol and 1,4-DMB. At the same time, the specific catalytic activity of Ni-SiO_2 and NiCu-SiO_2 in the TH of anisole remains relatively high compared to that of dimethoxybenzenes.

Thus, the high-loaded Ni-based catalysts synthesized using coprecipitation in supercritical CO_2 demonstrated excellent performance in the TH of the phenolic compounds. The significant influence of the structure of the phenolic compound on the catalytic activity was shown. In particular, the transformations of guaiacol were found to be the fastest due to the presence of the non-methylated OH group. In contrast to other dimethylbenzene position isomers, 1,3-DMB actively loses oxygen atoms, transforming into methoxycyclohexane

and cyclohexanol; however, the rate of its transformations remains the lowest compared to other isomers. There are many studies showing the positive effect of the Cu addition on the rate of the reductive transformations. This work demonstrates that in the case of TH of phenolic compounds, Cu can affect the rate constants in the different ways.

3. Materials and Methods

3.1. Materials

The following materials were used: 2-PrOH (≥99.8, EKOS-1), MeOH (J.T. Barker, Phillipsburg, NJ, USA, HPLC Gradient Grade), 1,2-dimethoxybenzene (99%, Sigma-Aldrich, Burlington, MA, USA), 1,3-dimethoxybenzene (≥98%, Sigma-Aldrich), 1,4-demethoxybenzene (99%, Sigma-Aldrich), guaiacol (≥98%, Sigma-Aldrich), dodecane (≥99%, Sigma-Aldrich), tetraethoxysilane (TEOS, 98%, Acros Organics, Geel, Belgium), $Ni(OAc)_2 \cdot 4H_2O$, (99% extra, Acros Organics), $Cu(OAc)_2 \cdot H_2O$, (98%, Sigma Aldrich), and CO_2 (99.8%, Promgazservis, Orenburg, Russia).

3.1.1. Catalyst Preparation and Characterization

The catalysts were synthesized according to the original supercritical antisolvent co-precipitation method using the SAS-50 setup (Waters, Milford, MA, USA). The obtained solid particles were characterized by XRD, XRF, TEM, EDX, and CO adsorption. The detailed procedure of the catalyst synthesis and characterization is described in our previous publication [25]. Two samples, Ni-SiO_2 and NiCu-SiO_2, were synthesized.

3.1.2. Batch Experiments

Before application in the treatment of the phenolic compounds, the Ni-based catalysts were reduced in H_2 flow (30 L/h) at 400 °C for NiCu-SiO_2 and at 450 °C for Ni-SiO_2, to obtain the metal nanoparticles. The completeness of the reduction process was controlled by XRD. After 45 min under H_2 flow, the catalysts were cooled down to room temperature. Then, H_2 was replaced with Ar, and catalyst was placed under 2-PrOH, avoiding contact with air.

The catalytic experiments were carried out in the batch reactor (285 mL, AISI 316 L). The system was purged with Ar and then charged by the reaction mixture, including a catalyst (0.10–0.11 g); 2-PrOH (110 mL); phenolic compound (30 mmol, 3.72–4.14 g); and dodecane (0.30 g), which was used as an internal standard. After charging, the reactor was purged with Ar under stirring (mechanical agitator MagneDrive®, Erie, PA, USA, 800 rpm), closed, and then heated up to 250 °C for 30–35 min. During the experiment, the pressure was 7.0–7.7 MPa, and no H_2 or any other substances were added to the reaction mixture. The probes were collected just after reaching the target temperature, and then after 20, 40, 60, 90, 120, and 180 min of the reaction. The conversion of the initial substrate and yield of the products was calculated according to the following equations:

$$Conversion = \left(1 - \frac{C^0_{ph} - C_{ph}}{C^0_{ph}}\right) \times 100\% \quad (1)$$

$$Yield = \frac{C_{pr}}{\sum C_{pr}} \times 100\% \quad (2)$$

where C^0_{ph} and C_{ph} represent molar concentrations of the phenolic compounds (guaiacol and dimethoxybenzenes) in the reaction mixture at an initial and a certain time, and C_{pr} represents a concentration of a certain product at a certain time.

3.1.3. Kinetic Calculations

The rate constants describing the consumption of phenolic compounds were calculated according to Equation (3):

$$\frac{dC_{ph}}{dt} = -(k - k_{ac} \times C_{ac}) \times C_{ph} \quad (3)$$

where C_{ph} is a concentration of the phenolic compound in the solution at a certain time, C_{ac} is a concentration of acetone in the solution at a certain time, k is the kinetic constant of phenolic compound consumption, and k_{ac} is a coefficient showing the proportion between acetone in the solution and on the catalyst surface.

3.1.4. Product Analysis

The liquid products were analyzed using the Shimadzu GCMS-QP2010 SE spectrometer (Kyoto, Japan), equipped with an autosampler. The GsBP-INOWAX capillary chromatographic column (crosslinked polyethylene glycol) was used (length 30 m, internal diameter 0.32 mm, and stationary phase thickness 0.25 μm). The column was conditioned at 55 °C for 3 min, heated up to 200 °C at a rate of 15 °C per minute, and then heated up to 250 °C at a rate of 25 °C per minute. The evaporator temperature was 270 °C, and helium was used as a carrier gas. The products were identified using the peak retention time and the mass spectrum of the substance, which were compared with the corresponding data of the pure compounds or with the data from the NIST and Wiley electronic mass spectral libraries. Conversion of the initial phenolic compound and the yield of the products were evaluated by the internal standard method using dodecane.

To determine the qualitative composition of the formed gases, the reactor was cooled to 40 °C when the pressure dropped to 1.3–2.0 MPa. Then, the gas was sampled from the reactor using a 150 mL syringe. Before the analysis, a gas sample in the syringe was diluted 20 times with air. The chromatographic analysis was preformed using a Chromos GC 1000 (Chromos, Nizhny, Russia) equipped with a chromatography column (length 2 m, internal diameter 3 mm, and stationary phase—NaX zeolite) and a thermal conductivity detector. Ar was used as a carrier gas, and the temperature mode of column conditioning was as follows: 30 °C for 3 min, programmed heating up to 120 °C at a rate 24 °C/min, and then for 5 min at 120 °C.

4. Conclusions

This study shows that high-loaded Ni and Ni-Cu catalysts demonstrate promising results in transformations of phenolic compounds and 2-PrOH under supercritical conditions. The obtained kinetic constants show the high reactivity of guaiacol compared to dimethoxybenzenes and the negative influence of Cu addition on the reaction rate. At the same time, Cu promotes transformations of 1,2-dimethoxybenzene, increasing the rate constant from 1.3×10^{-2} min^{-1} to 1.6×10^{-2} min^{-1}. Guaiacol and 1,3-dimethoxybenzene actively lose oxygen atoms, transforming into cyclohexanol and methoxycyclohexane, whereas the main products of 1,2-and 1,4-dimethoxybenzene transfer hydrogenation are corresponding dimethoxycyclohexanes. Thus, the copper addition and the structure of phenolic compounds significantly affect the rate and selectivity of transfer hydrogenation. This study expands the understanding of the fundamental aspects of H_2-free hydrogenation.

Supplementary Materials: The following supporting information can be downloaded at https://www.mdpi.com/article/10.3390/catal12121655/s1, Figure S1: XRD data obtained for the catalysts after activation in H_2. A—Ni-SiO_2, B—NiCu-SiO_2; Table S1: Content of Ni and Cu in the Ni-Cu catalysts measured by XRF. D—mean crystallite size, a—lattice parameter, measured by XRD, and S_{CO}—surface area, measured by CO adsorption.; Figure S2: TEM and EDX-mapping pictures obtained for A—Ni-SiO_2, B—NiCu-SiO_2; Figure S3: Kinetic data for the experiments with guaiacol over A—Ni-SiO_2 and NiCu-SiO_2. The first-order kinetic model was used; the dots—experimental data, and the lines—calculated using Equation (3); Figure S4: Kinetic data for the experiments

with 1,2-DMB over A—Ni-SiO_2 and NiCu-SiO_2. The first-order kinetic model was used; the dots—experimental data, and the lines—calculated using Equation (3); Figure S5: Kinetic data for the experiments with 1,3-DMB over A—Ni-SiO_2 and NiCu-SiO_2. The first-order kinetic model was used; the dots—experimental data, and the lines—calculated using Equation (3); Figure S6: Kinetic data for the experiments with 1,4-DMB over A–Ni-SiO_2 and NiCu-SiO_2. The first-order kinetic model was used— the dots–experimental data, and the lines—calculated using Equation (3).

Author Contributions: Conceptualization, methodology, validation, formal analysis, investigation, writing—original draft preparation, writing—review and editing, and funding acquisition, A.P. and N.N.; and writing—original draft preparation, writing—review and editing, supervision, project administration, and funding acquisition, O.M. All authors have read and agreed to the published version of the manuscript.

Funding: This research was funded by Russian Science Foundation grant number 21-73-00049, (https://rscf.ru/project/21-73-00049/ (accessed on 27 July 2021)).

Data Availability Statement: Not applicable.

Conflicts of Interest: The authors declare no conflict of interest.

References

1. Gilkey, M.J.; Xu, B. Heterogeneous catalytic transfer hydrogenation as an effective pathway in biomass upgrading. *ACS Catal.* **2016**, *6*, 1420–1436. [CrossRef]
2. Thanigaivel, S.; Priya, A.K.; Dutta, K.; Rajendran, S.; Sekar, K.; Jalil, A.A.; Soto-Moscoso, M. Role of nanotechnology for the conversion of lignocellulosic biomass into biopotent energy: A biorefinery approach for waste to value-added products. *Fuel* **2022**, *322*, 124236. [CrossRef]
3. Ke, L.; Wu, Q.; Zhou, N.; Xiong, J.; Yang, Q.; Zhang, L.; Wang, Y.; Dai, L.; Zou, R.; Liu, Y.; et al. Lignocellulosic biomass pyrolysis for aromatic hydrocarbons production: Pre and in-process enhancement methods. *Renew. Sustain. Energy Rev.* **2022**, *165*, 112607. [CrossRef]
4. Gnanasekaran, L.; Priya, A.K.; Thanigaivel, S.; Hoang, T.K.A.; Soto-Moscoso, M. The conversion of biomass to fuels via cutting-edge technologies: Explorations from natural utilization systems. *Fuel* **2023**, *331*, 125668. [CrossRef]
5. Scholze, B.; Meier, D. Characterization of the water-insoluble fraction from pyrolysis oil (pyrolytic lignin). Part I. PY-GC/MS, FTIR, and functional groups. *J. Anal. Appl. Pyrolysis* **2001**, *60*, 41–54. [CrossRef]
6. Xu, J.; Zhu, P.; El Azab, I.H.; Bin Xu, B.; Guo, Z.; Elnaggar, A.Y.; Mersal, G.A.M.; Liu, X.; Zhi, Y.; Lin, Z.; et al. An efficient bifunctional Ni-Nb_2O_5 Nanocatalysts for the hydrodeoxygenation of anisole. *Chin. J. Chem. Eng.* **2022**, *49*, 187–197. [CrossRef]
7. Shafaghat, H.; Rezaei, P.S.; Ashri Wan Daud, W.M. Effective parameters on selective catalytic hydrodeoxygenation of phenolic compounds of pyrolysis bio-oil to high-value hydrocarbons. *RSC Adv.* **2015**, *5*, 103999–104042. [CrossRef]
8. Shuai, L.; Luterbacher, J. Organic Solvent effects in biomass conversion reactions. *ChemSusChem* **2016**, *9*, 133–155. [CrossRef]
9. Shafaghat, H.; Tsang, Y.F.; Jeon, J.K.; Kim, J.M.; Kim, Y.; Kim, S.; Park, Y.K. In-situ hydrogenation of bio-oil/bio-oil phenolic compounds with secondary alcohols over a synthesized mesoporous Ni/CeO_2 catalyst. *Chem. Eng. J.* **2020**, *382*, 122912. [CrossRef]
10. Philippov, A.A.; Nesterov, N.N.; Pakharukova, V.P.; Martyanov, O.N. High-loaded ni-based catalysts obtained via supercritical antisolvent coprecipitation in transfer hydrogenation of anisole: Influence of the support. *Appl. Catal. A Gen.* **2022**, *643*, 118792. [CrossRef]
11. Park, Y.K.; Ha, J.M.; Oh, S.; Lee, J. Bio-oil upgrading through hydrogen transfer reactions in supercritical solvents. *Chem. Eng. J.* **2021**, *404*, 126527. [CrossRef]
12. Yfanti, V.L.; Lemonidou, A.A. Effect of hydrogen donor on glycerol hydrodeoxygenation to 1,2-propanediol. *Catal. Today* **2020**, *355*, 727–736. [CrossRef]
13. Chen, H.; Xu, Q.; Zhang, D.; Liu, W.; Liu, X.; Yin, D. Highly efficient synthesis of γ-valerolactone by catalytic conversion of biomass-derived levulinate esters over support-free mesoporous Ni. *Renew. Energy* **2021**, *163*, 1023–1032. [CrossRef]
14. Reddy Kannapu, H.P.; Mullen, C.A.; Elkasabi, Y.; Boateng, A.A. Catalytic transfer hydrogenation for stabilization of bio-oil oxygenates: Reduction of p-cresol and furfural over bimetallic Ni-Cu catalysts using isopropanol. *Fuel Process. Technol.* **2015**, *137*, 220–228. [CrossRef]
15. Philippov, A.A.; Chibiryaev, A.M.; Martyanov, O.N. Base-free transfer hydrogenation of menthone by sub- and supercritical alcohols. *J. Supercrit. Fluids* **2019**, *145*, 162–168. [CrossRef]
16. Shafaghat, H.; Kim, J.M.; Lee, I.G.; Jae, J.; Jung, S.C.; Park, Y.K. Catalytic hydrodeoxygenation of crude bio-oil in supercritical methanol using supported nickel catalysts. *Renew. Energy* **2019**, *144*, 159–166. [CrossRef]
17. Alekseev, E.S.; Alentiev, A.Y.; Belova, A.S.; Bogdan, V.I.; Bogdan, T.V.; Bystrova, A.V.; Gafarova, E.R.; Golubeva, E.N.; Grebenik, E.A.; Gromov, O.I.; et al. Supercritical fluids in chemistry. *Russ. Chem. Rev.* **2020**, *89*, 1337–1427. [CrossRef]
18. Kim, J.Y.; Park, J.; Kim, U.J.; Choi, J.W. Conversion of lignin to phenol-rich oil fraction under supercritical alcohols in the presence of metal catalysts. *Energy Fuels* **2015**, *29*, 5154–5163. [CrossRef]
19. Goto, M. Chemical recycling of plastics using sub- and supercritical fluids. *J. Supercrit. Fluids* **2009**, *47*, 500–507. [CrossRef]

20. Tang, Z.-R.; Edwards, J.K.; Bartley, J.K.; Taylor, S.H.; Carley, A.F.; Herzing, A.A.; Kiely, C.J.; Hutchings, G.J. Nanocrystalline cerium oxide produced by supercritical antisolvent precipitation as a support for high-activity gold catalysts. *J. Catal.* **2007**, *249*, 208–219. [CrossRef]
21. Nesterov, N.S.; Pakharukova, V.P.; Martyanov, O.N. Water as a cosolvent—Effective tool to avoid phase separation in bimetallic Ni-Cu catalysts obtained via supercritical antisolvent approach. *J. Supercrit. Fluids* **2017**, *130*, 133–139. [CrossRef]
22. Reverchon, E. Supercritical antisolvent precipitation of micro- and nano-particles. *J. Supercrit. Fluids* **1999**, *15*, 1–21. [CrossRef]
23. Nesterov, N.S.; Paharukova, V.P.; Yakovlev, V.A.; Martyanov, O.N. The facile synthesis of Ni-Cu catalysts stabilized in SiO_2 Framework via a supercritical antisolvent approach. *J. Supercrit. Fluids* **2016**, *112*, 119–127. [CrossRef]
24. Nesterov, N.S.; Smirnov, A.A.; Pakharukova, V.P.; Yakovlev, V.A.; Martyanov, O.N. Advanced green approaches for the synthesis of nicu-containing catalysts for the hydrodeoxygenation of anisole. *Catal. Today* **2021**, *379*, 262–271. [CrossRef]
25. Philippov, A.; Nesterov, N.; Pakharukova, V.; Kozhevnikov, I.; Martyanov, O. Advanced high-loaded Ni—Cu catalysts in transfer hydrogenation of anisole: Unexpected effect of Cu addition. *Catalysts* **2022**, *12*, 1307. [CrossRef]
26. De Castro, I.B.D.; Graça, I.; Rodríguez-García, L.; Kennema, M.; Rinaldi, R.; Meemken, F. Elucidating the reactivity of methoxyphenol positional isomers towards hydrogen-transfer reactions by ATR-IR spectroscopy of the liquid-solid interface of RANEY® Ni. *Catal. Sci. Technol.* **2018**, *8*, 3107–3114. [CrossRef]
27. Viar, N.; Requies, J.M.; Agirre, I.; Iriondo, A.; Gil-Calvo, M.; Arias, P.L. Ni-Cu bimetallic catalytic system for producing 5-hydroxymethylfurfural-derived value-added biofuels. *ACS Sustain. Chem. Eng.* **2020**, *8*, 11183–11193. [CrossRef]
28. Ganesan, M.; Liu, C.C.; Pandiyarajan, S.; Lee, C.T.; Chuang, H.C. Post-supercritical CO_2 electrodeposition approach for Ni-Cu alloy fabrication: An innovative eco-friendly strategy for high-performance corrosion resistance with durability. *Appl. Surf. Sci.* **2022**, *577*, 151955. [CrossRef]
29. Sequeira, C.A.C.; Cardoso, D.S.P.; Amaral, L.; Šljukić, B.; Santos, D.M.F. On the performance of commercially available corrosion-resistant nickel alloys: A review. *Corros. Rev.* **2016**, *34*, 187–200. [CrossRef]
30. Guo, Q.; Wu, M.; Wang, K.; Zhang, L.; Xu, X. Catalytic hydrodeoxygenation of algae bio-oil over bimetallic Ni-Cu/ZrO_2 catalysts. *Ind. Eng. Chem. Res.* **2015**, *54*, 890–899. [CrossRef]
31. Gao, B.; Zhang, J.; Yang, J.-H. Bimetallic Cu-Ni/MCM-41 catalyst for efficiently selective transfer hydrogenation of furfural into furfural alcohol. *Mol. Catal.* **2022**, *517*, 112065. [CrossRef]
32. Szczyglewska, P.; Feliczak-Guzik, A.; Nowak, I. Ordered mesoporous silica-supported metal catalysts for hydrodeoxygenation of anisole derivatives. *Microporous Mesoporous Mater.* **2021**, *312*, 110691. [CrossRef]
33. Ardiyanti, A.R.; Khromova, S.A.; Venderbosch, R.H.; Yakovlev, V.A.; Heeres, H.J. Catalytic hydrotreatment of fast-pyrolysis oil using non-sulfided bimetallic Ni-Cu catalysts on a δ-Al_2O_3 support. *Appl. Catal. B Environ.* **2012**, *117–118*, 105–117. [CrossRef]